MODIFICATION OF GRAPHENE OXIDE SURFACE BY DOPAMINE HYDROCHLORIDE

[1,2] Karel KLOUDA, [2]Petra ROUPCOVÁ, [3]Hana KUBÁTOVÁ, [2]Bohdan FILIPI, [4]David KRSEK, [1]Kateřina BÁTRLOVÁ

[1]Occupational Safety Research Institute, Prague, Czech Republic, EU,
klouda@vubp- praha.cz, batrlova@vubp-praha.cz;

[2] VSB - Technical University of Ostrava, Ostrava, Czech Republic, EU,
karel.klouda@vsb.cz, petra.roupcova@vsb.cz, bohdan.filipi@vsb.cz;

[3] State Office for Nuclear Safety, Prague, Czech Republic, EU, hana.kubatova@sujb.cz

[4]National Institute of Public Health, Prague, Czech Republic, EU, krsek@szu.cz;

Abstract

Polydopamine is an organic substance that is almost universally applicable to cover all kinds of materials, including nanomaterials. Considering the possible use of polydopamine in the water purification process, this article focuses on the change of selected properties of the chosen material (graphene oxide and the hybrid compound graphene oxide-C60) after being coated with polydopamine. Attention was paid to changes in thermal stability and surface morphology. In particular, changes in surface morphology could positively affect the sorption capabilities of the original materials in relation to organic pollutants.

Keywords: Metallurgy, steel, properties, applications, testing methods

1.   INTRODUCTION

Dopamine (DA) is a biologically active substance from the catecholamine group. It is a neurotransmitter that is naturally produced in the nervous system of humans and animals. At the same time, it can be easily synthetized in large quantities. It is easy to prepare polydopamine (PDA) from dopamine and other catecholamines, [1,2]. It is currently being studied in detail for its unique properties, which are very similar to the adhesive proteins of marine shells. Adhesive proteins allow mussels to interact with the substrate in moist environments, and they are rich in 3,4-dihydroxyphenylalanine (DOPA) as well as cysteine and lysine [1, 4]. The catechol side chain of DOPA is responsible for the strong bond between the surface of a bivalve leg and the substrate, as well as for the rapid solidification of the adhesive proteins. Catechol forms strong covalent and non-covalent interactions with the surface [5]. The synergistic effect of catechol and amine moiety further enhances biomolecular adhesion [1,3]. These strong interactions with surfaces are also generated by PDA. Therefore, PDA is seen as an organic substance that is almost universally applicable to cover all kinds of materials. The thickness of the PDA layer can be influenced by the reaction conditions (reaction time, temperature, pH) [1,5,6]. Following PDA application, new functional groups (mainly hydroxyl or other, depending on the pH) appear on the surface of a material increasing its hydrophilicity. These functional groups can be subsequently used for further surface modifications [3]. PDA demonstrates considerable chemical and environmental stability [7]. Pyrolysis at temperatures around 800 °C produces a material with a graphene-like structure, where a nitrogen atom is irregularly embedded in the carbon skeleton. The obtained material is electrically conductive [1,6]. PDA can be applied in many fields due to its potential to undergo further surface modifications and its ability to adhere to organic and inorganic substances. In biomedicine, for example, it is used to prepare nanocapsules for drug delivery or to reduce the immunogenicity of materials by improving their hydrophilicity and biocompatibility [8]. PDA can be widely used in wastewater treatment to remove heavy metals, organic pollutants, dyes and radioactive isotopes [9,10-12].

Our experiments focused specifically on the potential applications in water treatment. Graphene oxide (GO) [13,14] and its hybrid compounds [15,16] demonstrate sorption capabilities. It can be assumed that the reaction with DA will increase these abilities as a result of surface modification. Since we consider using both materials for sorption of organic pollutants present in water, it is necessary to have characteristics of both the input materials and of the materials with modified surfaces. For the pilot characterization we have chosen to use FTIR, TGA, DSC and microscopic methods (optical microscopy, TEM).

2. EXPERIMENTAL PART AND RESULTS

GO was prepared by oxidating finely ground graphite (0.025 mm) according to the classical Hummers method (H_2SO_4, $NaNO_3$, H_2O_2, $KMnO_4$, HCl) [17]. The oxidation product was repeatedly centrifuged until a negative reaction to sulfate ions was obtained. The prepared GO (0.389 g) was subsequently used for the reaction with dopamine hydrochloride (0.309 g). PDA was synthesized via DA self-polymerization. The reaction was carried out in water (30 ml) with an addition of hydrogen peroxide (30%; 0.4 ml). The suspension was agitated for 19 h and the pH was adjusted to 8-9 using $NaHCO_3$. The resulting suspension was washed with water and ethanol on a filter and then dried at 55 °C on a Petri dish. The hybrid compound GO-C_{60} (3:1) was prepared by the simultaneous oxidation of graphite with fullerene C_{60} in a weight ratio of 3:1. The procedure is described in Roupcová's dissertation [18]. The obtained GO-C_{60} (3:1) (0.350 g) was used for the reaction with dopamine hydrochloride (0.3 g). The reaction was carried out in water (30 ml) with an addition of hydrogen peroxide (30%; 0.4 ml) for 4 h. The pH was adjusted to 8-9 using $NaHCO_3$. The obtained suspension was washed with water and ethanol on a filter and then dried at 55 °C on a Petri dish.

2.1. Characterization of materials by FTIR

Fourier transform infrared spectroscopy (FTIR) of GO and GO-PDA in KBr pellets was conducted on Digilab Excalibur FTS 3000 MX model spectrometer (USA) with a scanning range of 4000-600 cm^{-1}. The obtained spectra are presented in **Figure 1**.
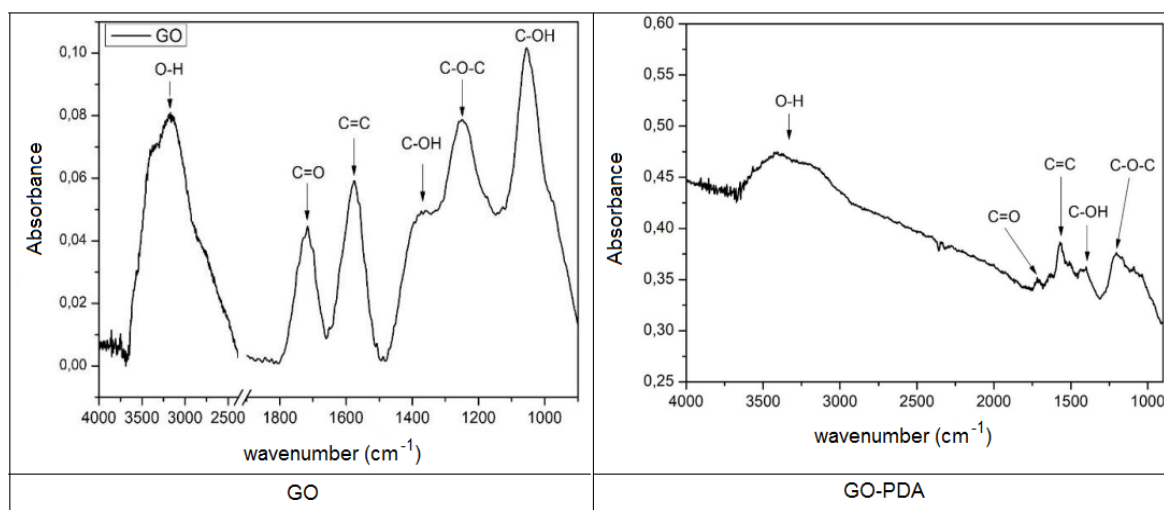
Figure 1 The FTIR spectra of GO and product formed on reaction of GO and PDA (GO-PDA)

The GO spectrum is characterized by intense bands indicating C=O valence vibrations (ketones and carboxylic acids, especially at the edges of graphitic structures), C=C (planar vibration of sp^2 hybridized bonds of the aromatic ring of unoxidized graphene), C-OH, C-O-C (epoxides) and C-OH (carboxylic acids) functional groups at 1720 cm^{-1}, 1575 cm^{-1}, 1380 cm^{-1}, 1250 cm^{-1} and 1055 cm^{-1}. The broad band in the region~ 3050 to 3700 cm^{-1} may be attributed to vibrations of O-H groups belonging to phenols, carboxylic acids and adsorbed water.

Although the spectrum of the GO-PDA product has different absorbance intensities, it also features characteristic vibration values for oxygen functional groups (1720 cm^{-1}, 1575 cm^{-1}, 1390 cm^{-1}, 1210 cm^{-1}, a broad band in the region $\sim$ 3050 to 3450 cm^{-1}). No significant absorbance bands were identified in the spectrum for C-N or N-H bonds which should be present in the broad band ($\sim$ 3050 to 3500 cm^{-1}). This is caused by the overlapping of contributions of different functional groups with similar absorption energies. The obtained results are consistent with those published by other teams [19, 20]. Insignificant peaks are visible at 1500 cm^{-1} and 1680 cm^{-1} which correspond to other characteristic bands for N-H and C-N bonds, respectively.

2.2. TGA and DSC analysis

2.2.1. TDA and DSC analysis of GO and GO-PDA

Thermogravimetric analysis (TGA) and differential scanning calorimetry (DSC) were performed on Mettler Toledo STAR^e, temperature range 25 – 750 °C (20 K/min, Air 50 ml/min). The decomposition was examined in air atmosphere. The thermal decomposition curves of GO are shown in **Figure 2**, and of GO-PDA in **Figure 3**. The GO decomposition showed one endothermic effect with the maximum at 77 ºC and two continuous exothermic effects [with the maximums at 236 ºC and 537 ºC]. The overall thermal effect of the composition is 13003 J/g. The thermal decomposition of the GO and DA product shown in **Figure 2** starts from 90 ºC with a slight exothermic effect which reaches the maximum at 207 ºC. From this maximum to 440 ºC there is a steady 9.73% decline, and the second exothermic effect begins with the maximum at 566 ºC. Its shape is a typical Gaussian curve. The weight loss of the sample at the second exothermic effect is 63.22 % and the overall thermal effect is 14590 J/g.
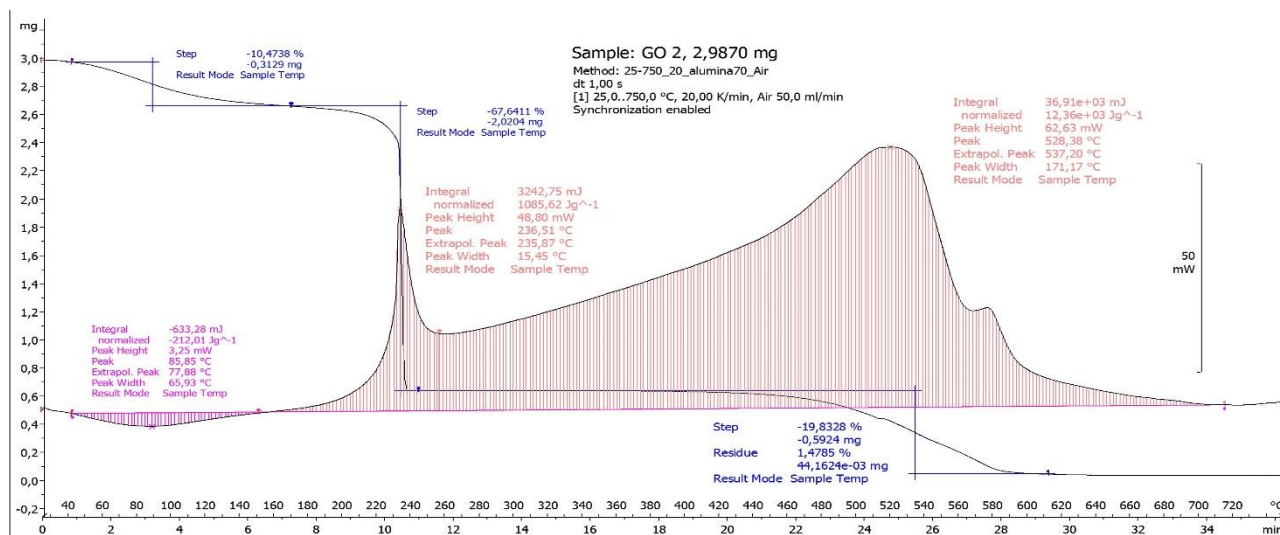
Figure 2 Thermal analysis data measured for GO (TGA/DSC curves)

2.2.2. TDA and DSC analysis of hybrid compounds GO-C$_{60}$ and GO-C$_{60}$ -PDA

In her thesis Roupcová reports that the hybrid compound GO-C$_{60}$ (3:1) decomposes with two exothermic effects. The maximum weight loss (51.1 %) occurs during the first exothermic effect (197 – 205 °C) with the maximum at 205 °C. The second exothermic effect occurs in the range 281-491 °C with the maximum at 390 °C (18 % weight loss) [14]. The thermal decomposition of GO-C$_{60}$ -PDA occurred essentially in two continuous exothermic effects (**Figure 4**). The maximum weight loss (48.1 %) occurred during the first part of the exothermic effect in the temperature range 215-380 °C. The second part of the exothermic effect followed in the 380-561 ºC range, with three maximums (430 °C, 456 °C and 470 °C) and with a cumulative weight loss of 32.7 %. The results described above indicate that the PDA coating increased the thermal stability of the original GO-C$_{60}$.
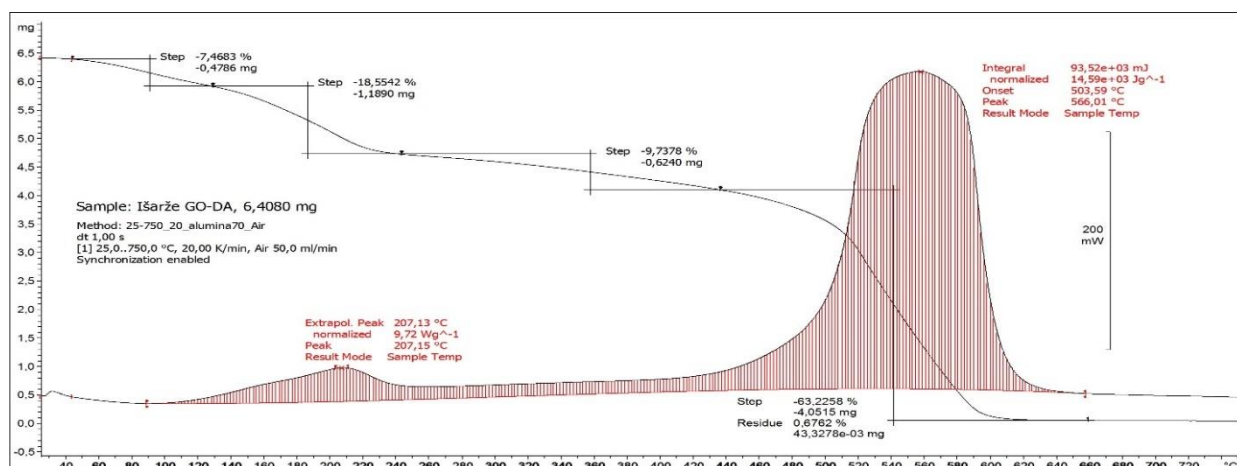
Figure 3 Thermal analysis data measured for GO-PDA (TGA/DSC curves)
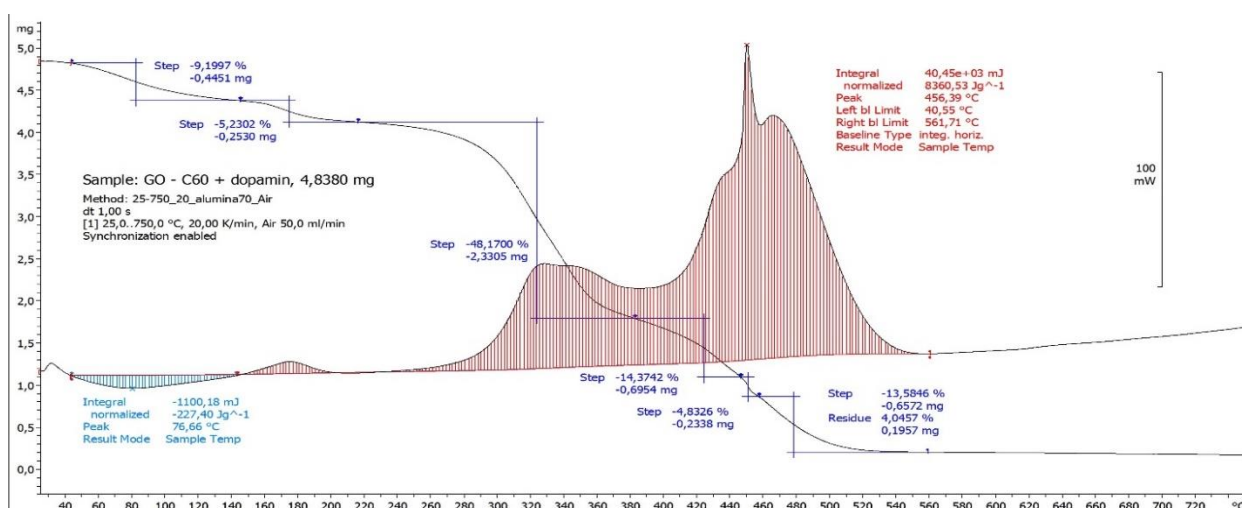
Figure 4 Thermal analysis data measured for GO-C_{60} -PDA (TGA/DSC curves)

2.3. Morphology

Microscopic images (Twist Digital Microscope, Learning Resources) of the dried suspension of GO and GO-PDA on a Petri dish show different surface morphologies of GO and GO after reaction with DA (GO-PDA) even at low magnification (20x) (**Figure 5**). The PDA coating increased the surface roughness. Transmission electron microscopy (TEM) (HT7800, Hitachi, accelerating voltage 100 kV) was used to investigate the GO-PDA and GO-C_{60} -PDA morphology. Nanoparticles present in the filtrate after filtration of prepared suspensions were used for the investigation. TEM image of GO-PDA and GO-C_{60} -PDA are shown in **Figure 6**. It is obvious that nanoparticles of both materials are mostly spherical in shape and form aggregates
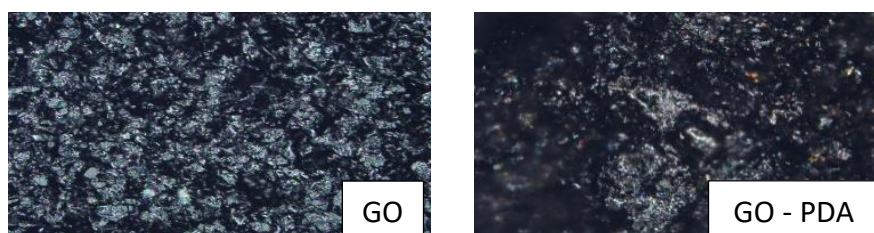
Figure 5 Microscopic images of the morphology of the initial GO (left) and the products of its reaction with DA (right) (magnification 20x)
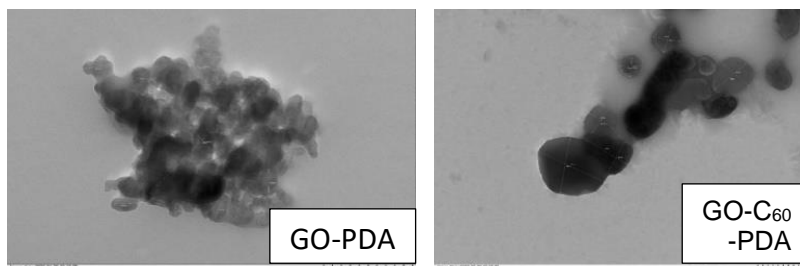
Figure 6 Transmission electron microscopy (TEM) images of GO-PDA (left) and GO-C_{60} -PDA (right)

3.   DISCUSSION AND CONCLUSION

The FTIR spectrum of GO contains well-resolved bands, which correspond to vibrations of individual types of bonds in the compound. The spectrum of GO-PDA is quite different. It is formed by broad bands that overlap. These bands correspond to different bond types and oxidation states, different cyclic structures (both heterocyclic and aromatic), and to a variety of bridging bonds and positions. The reason is the PDA structure. The PDA polymer consists of several various monomer units, which are diversely grouped and interconnected and are in different oxidation states [1]. The results of the GO thermal analysis are consistent with those obtained by other research teams [20,21]. The curves suggest that the reaction with DA resulted in a significant reduction of the epoxy bonds (C-O-C) present in both the initial GO and GO-C_{60}. The PDA covering also increased thermal stability of both the initial materials. The PDA covering resulted in a change of the surface morphology. As reported by Bogdan et al. [22], the PDA coating is always made up of two components. The first is a quasi-flat film with intrinsic roughness in the order of 1 nm. The second consists of PDA aggregates lying on top of this film. Larger aggregates can be easily separated by sonication. Therefore sonication may be used to achieve a more even covering and to reduce roughness [22]. Since the GO used in our experiments was not sonicated, we assume that this fact may have influenced the newly formed surface structures. Different monomer units or PDAs could have intercalated between the oxidized carbon layers of the initial graphite. As reported by previous research, thickness of the PDA layer can be influenced by reaction conditions (reaction time, temperature, pH) [1,5,6]. For example, Jia et al. [23] reported that the PDA layer may be up to 50 nm thick. Bogdan et al. [22] therefore suggest that morphological characteristics of PDA coverings should be evaluated based on an agreed standardized protocol. Based on the results of the performed experiments, we assume that the coverings of GO and of the hybrid compound GO-C_{60} changed their sorption properties. The introduction of novel functional groups will allow the formation of new non-covalent bonds with the surface of materials. Therefore the simultaneous use of initial materials and materials with a modified surface could expand the application potential of GO and its reduced forms.

ACKNOWLEDGEMENTS

REFERENCES

[1]   LIEBSCHER, J. Chemistry of Polydopamine - Scope, Variation, and Limitation. *Eur. J. Org. Chem.* 2019, vol. 31-32, pp. 4976-4994. Available from: https://doi.org/10.1002/ejoc.201900445.

[2]   BALL, V. Polydopamine Nanomaterials: Recent Advances in Synthesis Methods and Applications. *Front. Bioeng. Biotechnol.* 2018, vol. 6, no. 109. Available from: https://doi.org/10.3389/fbioe.2018.00109.

[3]   DELPARASTAN, P., MALOLLARI, K., G., HAESHIN, L., MESSERSMITH, P., B. Direct Evidence for the Polymeric Nature of Polydopamine. *Angew Chem Int Ed Engl.* 2019, vol. 58, no. 4, pp. 1077–1082. Available from: https://doi.org/10.1002/anie.201811763.

[4]   PETRONE, L., KUMAR A., SUTANTO C., PATIL N. J., KANNAN S., et al. Mussel adhesion is dictated by time-regulated secretion and molecular conformation of mussel adhesive proteins. *Nature Communications*. 2015, vol. 6, no. 8737. Available from: https://doi.org/10.1038/ncomms9737.

[5]   KORD-FOROOSHANI, P., POLEGA, E., THOMSON, K., BHUIYAN, MD. S. A., PINNARATIP, R., TROUGHT, M., KENDRICK, C., GAO, Y., PERRINE, K. A., PAN, L., LEE, B. P. Antibacterial Properties of Mussel-Inspired Polydopamine Coatings Prepared by a Simple Two-Step Shaking-Assisted Method. *Frontiers in Chemistry*, 2019, vol. 7, no. 631. Available from: https://doi.org/10.3389/fchem.2019.00631.

[6]   LI, H., XI, J., DONAGHUE, A. G., KEUM, J., ZHAO. Y., AN, K., MCKENZIE, E. R., FEI, R. Synthesis and catalytic performance of polydopamine supported metal nanoparticles. *Scientific Reports*. 2020, vol. 10, 10416. Available from: https://doi.org/10.1038/s41598-020-67458-9.

[7]   HUANG, X., Qiao K., LI, L., LIU, G., XU, X., LU, R., GAO, H., XU, D. Preparation of a magnetic graphene/polydopamine nanocomposite for magnetic dispersive solid-phase extraction of benzoylurea insecticides in environmental water samples. *Scientific Reports*. 2019, vol. 9. Available from: https://doi.org/10.1038/s41598-019-45186-z.

[8]   YAN, J., WU, R., LIAO, S., JIANG, M., QIAN, Y. Applications of Polydopamine-Modified Scaffolds in the Peripheral Nerve Tissue Engineering. *Front Bioeng Biotechnol*. 2020, vol. 8. Available from: https://doi.org/10.3389/fbioe.2020.590998.

[9]   YAN, Z., ZHANG, Y., YANG, H., FAN, G., DING, A., LIANG, H., LI, G., REN, N., VAN DER BRUGGEN, B. Mussel-inspired polydopamine modification of polymeric membranes for the application of water and wastewater treatment: A review. *Chemical Engineering Research and Design*. 2020, vol. 157, no. 1, pp. 195-214. Available from: https://doi.org/10.1016/j.cherd.2020.03.011.

[10]   FREEMAN, B. D., PARK, H. B., MCCLOSKEY, B. D. Water purification membranes with improved fouling resistance. EP 2 318 126 B1. 2018. https://patentimages.storage.googleapis.com/33/0c/cc/6961954db14ff0/EP2318126B1.pdf

[11]   KONG, F., LIU, Q., YOU, L., LU, P., LIU, T., SUN, G., WANG, Y., CHEN, J. Facile preparation of dopamine mediated graphene oxide composite membranes with enhanced stability for nanofiltration: structure, performance and stability. *Desalination*. 2022, vol. 534. Available from: https://doi.org/10.1016/j.desal.2022.115778.

[12]   LEE, J., PATEL, R. Wastewater Treatment by Polymeric Microspheres: A Review. *Polymers*. 2022, vol. 14, no. 9. 1890. Available from: https://doi.org/10.3390/polym14091890.

[13]   WEI, D., ZHAO, C., KHAN, A., SUN, L., JI, Y., AI, Y., WANG, X. Sorption mechanism and dynamic behavior of graphene oxide as an effective adsorbent for the removal of chlorophenol-based environmental-hormones: A DFT and MD simulation study. *Chemical Engineering Journal*. 2019, vol. 375. Available from: https://doi.org/10.1016/j.cej.2019.121964.

[14]   BUELKE, Ch., ALSHAMI, A., CASLER, J., LEWIS, J., AL-SAYAGHI, M., HICKNER, M. A. Graphene oxide membranes for enhancing water purification in terrestrial and space-born applications: state of the art. *Desalination*. 2018, vol. 448, pp. 113-132. ISSN 00119164. Available from: https://doi.org/10.1016/j.desal.2018.09.008.

[15]   PAKULSKI, D., GORCZYŃSKI, A., MARCINKOWSKI, D., et al. High-sorption terpyridine-graphene oxide hybrid for the efficient removal of heavy metal ions from wastewater. *Nanoscale*. 2021, vol. 13, pp. 10490-10499. Available from: https://doi.org/10.1039/D1NR02255E.

[16]   ROUPCOVÁ, P., KUBATOVÁ, H., KLOUDA, K., SLIVKOVÁ, S. Preparation and modification of hybrid compounds based on GO-Biochar and verification of their sorption properties. *Chemical Engineering Transaction*. 2021, vol. 84, pp. 61-66. Available from: https://doi.org/10.3303/CET2184011.

[17]   HUMMERS, W. S., OFFEMAN, R. E. Preparation of Graphitic Oxide. *Journal of the American Chemical Society*. 1958, vol. 80, no. 6, pp. 1339-1339. Available from: https://doi.org/10.1021/ja01539a017.

[18]   ALKHOUZAAM, A., QIBLAWEY, H., KHRAISHEH, M. Polydopamine Functionalized Graphene Oxide as Membrane Nanofiller: Spectral and Structural Studies. *Membranes*. 2021, vol. 11, no. 86. Available from: https://doi.org/10.3390/membranes11020086.

[19]   ROUPCOVÁ, Petra. Monitoring of the ecotoxicity of the carbon based nanoparticles. Ostrava, 2018. Disertation Thesis. VSB - Technical university of Ostrava, Faculty of Safety Engineering.

[20]   HU, W., HE, G., ZHANG, H., WU, X., LI, J., ZHAO, Z., QIAO, Y., LU, Z., LIU, Y., LI, C. M. Polydopamine-functionalization of graphene oxide to enable dual signal amplification for sensitive surface plasmon resonance

imaging detection of biomarker. *American Chemical Society*. 2014, vol. 86, no. 9, pp. 4488-93. Available from: https://doi.org/10.1021/ac500390.5.

[21]   SHTEIN, M., PRI-BAR, I., VARENIK, M., REGEV, O. Characterization of Graphene-Nanoplatelets Structure via Thermogravimetry. *Analytical Chemistry*. 2015, vol. 87, no. 8, pp. 4076-4080. Available from: https://doi.org/10.1021/acs.analchem.5b00228.

[22]   BOGDAN, D., GROSU, I. G., FILIP C. How thick, uniform and smooth are the polydopamine coating layers obtained under different oxidation conditions? An in-depth AFM study. *Applied Surface Science*. 2022, vol. 597. Available from: https://doi.org/10.1016/j.apsusc.2022.153680.

[23]   JIA, L., HAN, F., WANG, H., et al. Polydopamine-assisted surface modification for orthopaedic implants. *Journal of Orthopaedic Translation*. 2019, vol. 17, pp. 82-95. Available from: https://doi.org/10.1016/j.jot.2019.04.001.